Configuration interaction study of the single-electron transport in the vertical gated quantum dot

J. Adamowski[*], **S. Bednarek,** and **B. Szafran**

Faculty of Physics and Nuclear Techniques, University of Mining and Metallurgy (AGH), Kraków, Poland

Dedicated to Professor Jozef T. Devreese on the occasion of his 65th birthday

A theoretical description is presented for a single-electron transport through a vertical gated quantum dot. Using the configuration interaction method we study the correlation effects in the gated quantum dots. We have found that the electron-electron correlation only slightly changes the single-electron tunnelling conditions in the absence of an external magnetic field, but has a pronounced influence on the magnetic-field induced phase transitions in few-electron systems confined in quantum dots.

1 Introduction In a vertical gated quantum dot (QD) [1–3], a current between a source and drain is controlled by a third electrode (gate). If the gate voltage applied is sufficient to empty the QD from excess charge carriers, a small source-drain voltage causes that the single electrons can flow through the nanodevice. The resulting source-drain current is tuned by the gate voltage. This means that the nanodevice [1, 2], which contains the gated QD, can be treated as a prototype of a single-electron transistor. Only at certain well-defined gate-voltage values the subsequent electrons tunnel via the QD. Therefore, the single-electron transistor – as opposite to the conventional transistor – can be switched on and turned off at different gate-voltage values.

The conditions of the single-electron tunnelling via the QD are determined by the electrochemical potentials of the leads and the QD. The later is simply equal to the chemical potential (μ_{N+1}) of the N-electron system confined in the QD (artificial atom), which is defined as the difference between the ground-state energies of the $(N + 1)$- and N-electron systems, i.e.

$$\mu_{N+1} = E_{N+1} - E_N . \tag{1}$$

The single electron can tunnel from the source with electrochemical potential μ_s through the QD, that confines the N excess electrons, to the drain with electrochemical potential μ_d under the following condition:

$$\mu_s \geq \mu_{N+1} \geq \mu_d . \tag{2}$$

If condition (2) is fulfilled, we are speaking about an opening of the transport window. In the gated QDs, the typical values of the few-electron ground-state energies are of the order of mili-electronvolts. In order to determine the gate voltage, which will cause the single-electron tunnelling, with the re-

---

[*] Corresponding author: e-mail: adamowski@ftj.agh.edu.pl

quired precision, we need to know the N-electron energies with the uncertainty, which does not exceed a small fraction of meV. Therefore, we are dealing with the many-electron problem, which has to be solved with a high precision. For the N-electron system the computational accuracy depends on how exactly we can determine the potential confining the electrons in the QD and calculate the N-electron energy. In our recent paper [4], we have elaborated a self-consistent method for solving the underlying Poisson–Schrödinger problem. In particular, the method [4] allowed us to calculate accurately the confinement potential from the first principles of electrostatics. The confinement potential appears to be a complex function of the gate voltage and number of electrons in the QD [4]. In Refs. [4, 5], the Schrödinger equation has been solved by the Hartree-Fock method, which neglects the electron–electron correlation. The results [4] show a good agreement with experimental data in the absence of a magnetic field, but systematic deviations of the theoretical results [5] from the experimental data [1, 2] appear in the external magnetic field.

In the present paper, we extend the approach of Ref. [4] by applying the configuration interaction (CI) method, which allows us to include the electron–electron correlation. We will study the influence of correlation on the single-electron tunnelling conditions both with and without an external magnetic field.

The paper is organized as follows: in Section 2, for the sake of completeness, we briefly describe the self-consistent method [4] of solution of the Poisson–Schrödinger problem, in Section 3, we introduce the present CI approach, Section 4 contains the results, and Section 5 – the discussion and conclusions.

2 Self-consistent solution of the Poisson–Schrödinger problem   The model nanodevice used in the present calculations is depicted in Fig. 1. We put the boundary conditions on the surface shown by the dashed line and solve the Poisson equation in the entire nanodevice with the QD region included.

The electrostatic field confining the excess electrons in the InGaAs QD is created by source, drain, and gate electrodes, and ionized donor centers in n-GaAs layers. If there are N electrons, which are localized in the QD occupying the atomic-like bound states, the confined charge creates the additional electric field, which acts on the donors in the n-GaAs layers causing their ionization. This in turn changes the net electrostatic field in the QD and the quantum states of the QD-confined electrons. Therefore, the problem of the gated QD has to be solved self-consistently. A further complication
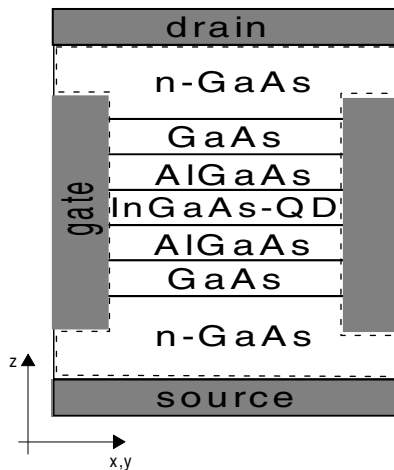
Fig. 1 Model nanostructure used in our calculations. Dashed line corresponds to the cross section of the surface, on which we put the boundary conditions for the Poisson equation.
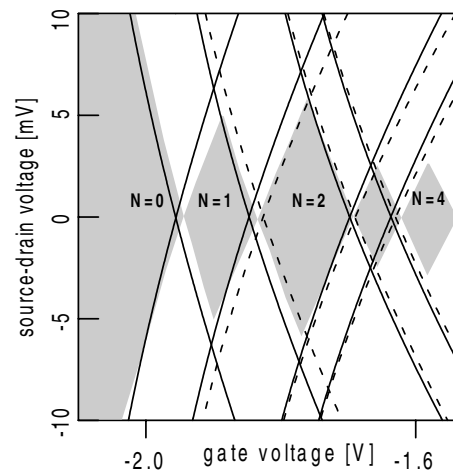
Fig. 2 Stability diagram with Coulomb diamonds at zero magnetic field. The measured [2] differential conductance is nearly zero in the grey areas. Solid (dashed) lines show the boundaries of the transport windows calculated by the CI (HF) method. The number of electrons (N) is fixed in each Coulomb blockade region.

results from the fact that – even for a homogeneous distribution of the impurity centers in the n-GaAs layers – the distribution of the ionized donors is inhomogeneous and depends on the number of electrons confined in the QD [4].

The confinement potential is the sum of the double-barrier potential, which stems from the conduction-band offsets and confines the excess electrons in the vertical (z) direction, and the electrostatic potential $\varphi_1(\boldsymbol{r})$, which is responsible for the lateral confinement of the electrons in the QD. Potential $\varphi_1(\boldsymbol{r})$ can be found from the Poisson equation

$$\nabla^2 \varphi_1(\boldsymbol{r}) = -\varrho_D(\boldsymbol{r})/\varepsilon_0 \varepsilon_s \,, \tag{3}$$

where $\varrho_D(\boldsymbol{r})$ is the space charge density, which originates from the ionized donors in the n-GaAs layers, and ε_s is the static dielectric constant of GaAs. The electrostatic field in the entire nanodevice can be determined, if we take into account the additional electrostatic potential $\varphi_2(\boldsymbol{r})$, which is created by the N electrons confined in the QD. The QD-confined electrons exert outside the QD the electrostatic field with the Hartree-type potential

$$\varphi_2(\boldsymbol{r}) = -\frac{\kappa e}{\varepsilon_s} \int d^3 r' \frac{\varrho_e(\boldsymbol{r}')}{|\boldsymbol{r} - \boldsymbol{r}'|} \,, \tag{4}$$

where $\kappa = 1/4\pi\varepsilon_0$ and $\varrho_e(\boldsymbol{r})$ is the confined electron charge density. According to the superposition principle, the total electrostatic potential in the nanodevice is the sum

$$\Phi_{\text{tot}}(\boldsymbol{r}) = \varphi_1(\boldsymbol{r}) + \varphi_2(\boldsymbol{r}) \,. \tag{5}$$

Charge density ϱ_D in Eq. (3) can be determined as follows [4]. In the low-temperature regime, in which the experiments [1,2] were performed, the thermal ionization of the donors can be neglected. In this case, the donors become ionized under the action of the electrostatic field with potential (5). In the nanodevice [1], the source and drain electrodes form ohmic contacts with the n-GaAs layers of the modulated doping. Therefore, the donor energy level is aligned with the electrochemical potential of the source (μ_s) at the source side of the nanodevice and that of the drain (μ_d) at the drain side. The ionization of the donor center at position $\boldsymbol{r}$ in the n-GaAs layer occurs if the total potential energy of the electron in the electrostatic field with potential (5), i.e.

$$U_{\text{tot}}(\boldsymbol{r}) = -e\Phi_{\text{tot}}(\boldsymbol{r}) \,, \tag{6}$$

exceeds the energy of the electron bound to the donor center, i.e. the corresponding electrochemical potential. This leads to the following donor ionization condition:

$$U_{\text{tot}}(\boldsymbol{r}) > \mu_{s(d)} \tag{7}$$

for the source (s) and drain (d) side of the nanodevice. Condition (7) allows us to determine the charge density ϱ_D in the following self-consistent manner: if condition (7) is fulfilled, then $\varrho_D(\boldsymbol{r}) = en_D(\boldsymbol{r})$, and $\varrho_D(\boldsymbol{r}) = 0$ otherwise, where $n_D(\boldsymbol{r})$ is the donor concentration in the n-GaAs layer.

The boundary conditions for the Poisson Eq. (3) are put on the total potential (5) and the boundary values of the potential φ_1 needed to solve Eq. (3) are calculated from Eq. (5). For the source and drain the corresponding boundary conditions have the form

$$\Phi_{\text{tot}}(\boldsymbol{r}_{s(d)}) = V_{s(d)} \,, \tag{8}$$

where V_s (V_d) is the source (drain) potential. At the gate surface, we take into account the Schottky barrier of height ϕ_B, which leads to the following boundary condition:

$$\Phi_{\text{tot}}(\boldsymbol{r}_g) = V_g - \phi_B/e \,, \tag{9}$$

where V_g is the gate voltage. According to Ref. [4], throughout the present paper, we take the common electrochemical potential of the source and drain in the absence of external fields (Fermi energy) as the reference energy.

Due to the cylindrical symmetry of the nanodevice [1], the Poisson Eq. (3) has been solved in cylindrical coordinates (ρ, z). The numerical solutions [4] show that the lateral (ρ) dependence of the

confinement potential is approximately parabolic. However, the non-parabolic corrections have to be taken into account in the QD regions located farther from the cylinder axis [4].

3 Configuration interaction method   We consider the N-electron artificial atom in an external magnetic field. In order to find the ground-state E_N, we have to solve the N-electron eigenproblem with the Hamiltonian

$$H = \sum_{i=1}^{N} h(\boldsymbol{r}_i) + \sum_{i=1}^{N} \sum_{j>i}^{N} \frac{\kappa e^2}{\varepsilon_\infty |\boldsymbol{r}_i - \boldsymbol{r}_j|}\,, \tag{10}$$

where ε_∞ is the high-frequency dielectric constant of the GaAs, which is responsible for the screening of the electron−electron interaction [6]. In Eq. (10), $\boldsymbol{r}_i$ are the position vectors of electrons and h is the single-electron Hamiltonian, which in the symmetric gauge reads

$$h(\boldsymbol{r}) = -\frac{\hbar^2}{2m_e}\nabla^2 + U_{\mathrm{conf}}(\boldsymbol{r}) + \frac{1}{8}\,m_e\omega_c^2(x^2+y^2) + \frac{1}{2}\,\hbar\omega_c l_z\,, \tag{11}$$

where m_e is the electron effective mass, $\omega_c = eB/m_e$ is the cyclotron frequency in magnetic field B, and l_z is the z component of the angular momentum operator. The confinement potential energy is given by

$$U_{\mathrm{conf}}(\boldsymbol{r}) = -e\varphi_1(\boldsymbol{r}) + U_{\mathrm{db}}(z)\,, \tag{12}$$

where $U_{\mathrm{db}}(z)$ is the potential energy of the electron in the double-barrier GaAs/AlGaAs/InGaAs layer structure. In the present paper, we apply the following one-electron wave functions:

$$\psi(\boldsymbol{r}) = \sum_{k_x,k_y=0}^{k_x+k_y\leq k} c_{k_x k_y} x^{k_x} y^{k_y} \exp\left[-\alpha(x^2+y^2) - \beta z^2\right]\,, \tag{13}$$

as the basis wave functions, where α and β are the non-linear and $c_{k_x k_y}$ the linear variational parameters. In the vertical gated QD, the electrons are confined in the vertical (z) direction much more strongly than in the ($x-y$) plane. Therefore, in Eq. (13), we choose a single z-dependent Gaussian, which is sufficient for a description of this motion, since all the confined electrons occupy the ground state of the quantized motion in the z direction. In the calculations, we exploit the property of the eigenstates of Hamiltonian (10), which possess the definite z components of the total angular momentum and total spin.

One-electron wave functions (13) are used to construct the Slater determinants with the required spin-orbital symmetry. In the framework of the CI method, the Slater determinants serve as a basis for the diagonalization of the N-electron Hamiltonian (10). In this paper, we consider $N = 1,\ldots,4$ electrons with the maximum value of the total angular-momentum quantum number $L_{\mathrm{max}} = 6$. The actual number of Slater determinants, used in the calculations, depends on the number of electrons N, total angular momentum L, and total spin S. For example, for $N = 4$, $L = 0$, $S = \hbar$, and $k = 5$ we take into account 2174 Slater determinants. According to the test calculations we performed, we obtain an accuracy of a few hundredth of meV for the ground-state energy. We have introduced the CI method into the self-consistent procedure of solving the Poisson−Schrödinger problem as follows. When solving the Poisson Eq. (3), we are still using the Hartree potential [Eq. (4)], in which the confined charge density ϱ_e is taken from the Hartree−Fock (HF) solution of the Schrödinger equation. The CI method is only used to calculate the ground-state energy of the N-electron system confined in the QD, i.e. to the solution of the Schrödinger equation with Hamiltonian (10).

4 Results   The stability diagram with the Coulomb diamonds is displayed in Fig. 2. The grey diamond-shaped areas correspond to the measured [2] Coulomb blockade regimes of the gate and source−drain voltages. In the transport measurements [2], the differential conductance is nearly zero within the Coulomb diamonds and takes on appreciable values in the white areas. The solid (dashed)
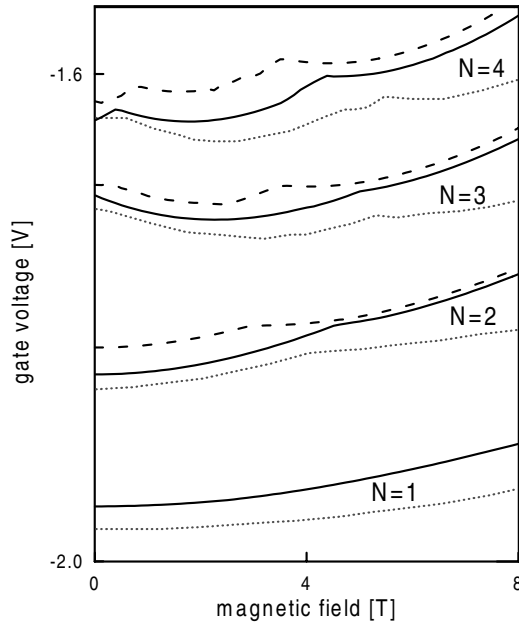
Fig. 3 Gate voltage corresponding to the current peaks as a function of magnetic field and number N of electrons confined in the QD. Solid, dashed, and dotted curves show the CI, HF, and experimental results, respectively.

lines show the boundaries of the Coulomb diamonds calculated by the CI (HF) method. We note that the results obtained by the CI and HF methods are very similar. They are significantly different only for the right limits of the first diamond ($N = 1$) and the left limits of the second diamond ($N = 2$). This difference results from the fact that the largest difference between the chemical potentials calculated by the CI and HF methods appears for $N = 2$. According to (2) chemical potential μ_2 determines the single-electron tunnelling in this region. Nevertheless, both the HF and CI methods lead to results, which reproduce the experimental data, with sufficient accuracy. In particular, this means that the HF method works surprisingly well for the gated QD. Small differences between the computational and experimental results can be ascribed to some simplifications of the theoretical model, e.g. the real QD can exhibit a certain deviation from the ideal cylindrical symmetry.

Single-electron transport via a gated QD is very sensitive to an external magnetic field [1, 2]. Figure 3 shows both the results of measurements [1, 2] and the present calculations. We see that the results of the CI method (solid curves) are in a better agreement with experiment than those of the HF method (dashed curves). This means that the correlation, which is included in the CI method and neglected in the HF method, has a pronounced effect on the results in the presence of a magnetic field. In Fig. 3, the cusps in the curves correspond to magnetic-field induced ground-state transformations in the confined N-electron system [5]. The HF method underestimates the critical magnetic fields for these transformations.

5 Discussion and conclusions Single-electron tunnelling via gated QD depends on the chemical potential of the artificial atom. According to (2) this chemical potential is the difference between the ground-state energies of the $(N + 1)$- and N-electron systems. If both the E_N and E_{N+1} are calculated with a comparable precision, the possible errors cancel out during the subtraction and chemical potential μ_N can be calculated quite accurately. This explains why the HF method leads to fairly good results for the Coulomb diamonds (Fig. 2). The improvement obtained by the more exact CI method is rather small. The magnetic-field induced phase transitions observed in the single-electron transport are more sensitive to the electron−electron correlation. In particular, the critical-field values are much better reproduced if we include the correlation by the CI method. This results from the fact that the critical magnetic fields are determined by the ground-state energy E_N rather than by the chemical potential μ_N and the HF errors do not cancel out.

The external magnetic field changes the donor energy according to the formula

$$E_D(B) = E_D(0) + \Delta E_D(B) \,, \tag{14}$$

where $E_D(0)$ is the ground-state donor energy for $B = 0$. In the magnetic-field regime $B \in [0, \, 8 \, \text{T}]$, the magnetic-field dependent shift of the donor ground-state energy can be expressed as follows:

$$\Delta E_D(B) = \lambda_1 B + \lambda_2 B^2 + \lambda_3 B^3 \,, \tag{15}$$

where the values of the coefficients $\lambda_1 = 0.01988$ T^{-1}, $\lambda_2 = 0.05983$ T^{-2}, and $\lambda_3 = -0.00252$ T^{-3} have been obtained from the accurate numerical solution of the donor problem in the magnetic field. In Eq. (15), the energy is measured in meV and magnetic field in tesla (T). We note that Eqs. (14) and (15) provide the corrected version of formula (5) in Ref. [5].

In the nanodevice [1], the electrochemical potentials of the source and drain determine the positions of the donor energy levels in the n-GaAs layers. In the single-electron transport measurements [1, 2], all the voltages are kept fixed. This means that the magnetic-field induced change of the electrochemical potential of the source (drain) by $\Delta E_D(B)$ is accompanied with the same change of the electrochemical potential of the gate. This in turn leads to the corresponding shift of the confinement-potential well bottom and – as a consequence – of all the energies, which enter into both the conditions of the single-electron transport (2) and donor ionization (7). As a result, conditions (2) and (7) should not be changed by the magnetic field. In Ref. [5], we have taken into account the magnetic-field induced shift of the donor energy in the tunnelling conditions. However, the corrections taken into account were very small. Therefore, the results of Ref. [5] exhibit negligibly small deviations from the present HF results (Fig. 3).

Let us comment on the applicability of the present stationary approach to the dynamic single-electron tunnelling process. The single-electron tunnelling conditions (2) with the equality signs determine the borders between the subsequent Coulomb blockade regions (cf. Fig. 2). The Coulomb blockade in QDs is associated with the formation of the stationary state of the N-electron artificial atom. If the gate voltage and/or the drain-source voltage cross the borders determined by condition (2), the number of QD-confined electrons changes as either $N \rightarrow N + 1$ or $N + 1 \rightarrow N$. Then, the confined electron system makes an abrupt transition to the stationary state of another system with the number of confined electrons changed by one. This allows us to determine the positions of the current peaks from conditions (2) with the equality signs. We note that the single-electron tunnelling is a spectroscopic tool applied to the artificial atoms, which is similar to the conventional optical spectroscopy for the natural atoms. The single-electron tunneling via the QD is an analog of the capture of the electron and the subsequent ionization of the natural atom. In particular, the addition energy, defined as the difference $\Delta\mu_N = \mu_{N+1} - \mu_N$, is an analog of the difference between the ionization energy and electron affinity [3].

There were several theoretical attempts [7−11] to describe the single-electron transport in the vertical gated QD [1]. The self-consistent solution of the Poisson and Schrödinger equations was presented in Ref. [7]. However, the authors [7] obtained only qualitative agreement with experiment [1]. The CI calculations for the vertical QDs [1] were performed by Eto [8], who assumed a fixed parabolic confinement potential. The assumption of the gate-voltage independent confinement potential did not allow him to describe the single-electron transport in the gated QD in a quantitative manner. Also in other theoretical papers [9−11] on gated QDs, the confinement potential was assumed of a fixed parabolic form. The results of our papers [4, 5] show that the dependence of the confinement potential on the gate voltage and number of confined electrons is crucial for the quantitative description of the electronic properties of the gated QD's.

In summary, in the present paper, we have included the CI method into our self-consistent procedure of solving the Poisson−Schrödinger problem for the vertical gated QDs. We have shown that electron−electron correlation plays an important role in the single-electron transport in an external magnetic field.

References

[1] S. Tarucha, D. G. Austing, T. Honda, R. J. van der Hage, and L. P. Kouwenhoven, Phys. Rev. Lett. **77**, 3613 (1996).
[2] L. P. Kouwenhoven, T. H. Oosterkamp, M. W. S. Danoesastro, M. Eto, D. G. Austing, T. Honda, and S. Tarucha, Science **278**, 1788 (1997).

[3] L. P. Kouwenhoven, D. G. Austing, and S. Tarucha, Rep. Prog. Phys. **64**, 701 (2001).
[4] S. Bednarek, B. Szafran, and J. Adamowski, Phys. Rev. B **64**, 195303 (2001).
[5] B. Szafran, S. Bednarek, and J. Adamowski, Phys. Rev. B **65**, 035316 (2002).
[6] S. Bednarek and J. Adamowski, Phys. Rev. B **57**, 14729 (1998).
[7] P. Matagne, J.-P. Leburton, J. Destine, and G. Cantraine, J. Compu. Model. Eng. Sci. **1**, 1 (2000).
    P. Matagne and J.-P. Leburton, Phys. Rev. B **65**, 235323 (2002).
[8] M. Eto, Jpn. J. Appl. Phys. **36**, 3924 (1997).
[9] M. Koskinen, M. Manninen, and S. M. Reimann, Phys. Rev. Lett. **79**, 1389 (1997).
[10] O. Steffens, U. Rössler, and M. Suhrke, Europhys. Lett. **42**, 529 (1998).
[11] T. F. Jiang, X.-M. Tong, and S.-I. Chu, Phys. Rev. B **63**, 045317 (2001).